

Plasma Confinement in an RF-driven Tandem Mirror with a Strong Temperature Anisotropy

ICHIMURA Makoto, CHO Teruji, HIGAKI Hiroyuki, HIRATA Mafumi, HOJO Hitoshi, ISHII Kameo, ITAKURA Akiyosi, KATANUMA Isao, KAWAMORI Eiji, KOHAGURA Jyunko, NAKASHIMA Yousuke, OKAMOTO Yuji, SAITO Teruo, TATEMATSU Yoshinori, YATSU Kiyoshi and YOSHIKAWA Masashi
Plasma Research Center, University of Tsukuba, Tsukuba, Ibaraki 305-8577, Japan

(Received: 12 December 2001 / Accepted: 2 August 2002)

Abstract

In the GAMMA 10 tandem mirror, the axial transport by the excitation of the Alfvén ion cyclotron (AIC) mode due to strong temperature anisotropy is discussed. The AIC modes are spontaneously excited in the high beta plasmas with a strong temperature anisotropy. The amplitude of the modes can be controlled by changing the cyclotron resonance conditions. The increase of the line density and anisotropy are affected by the excitation of the AIC modes. A resonant interaction between electrons and the AIC modes are observed in the end-loss energy analyzer. Pitch angle scattering of high energy ions trapped magnetically in the central cell and the enhancement of the end loss of high energy ions are also observed experimentally.

Keywords:

tandem mirror, ICRF, ECH, axisymmetrization, temperature anisotropy, AIC mode, axial transport, radial transport, high energy ion, pitch angle scattering

1. Introduction

The high density plasma production and confinement with electrostatic potentials are the major important issues in the present tandem mirror experiments [1,2]. In the GAMMA 10 tandem mirror, the ion cyclotron range of frequency (ICRF) heating and the electron cyclotron resonance heating (ECH) are used for the plasma production and heating, and for the potential formation, respectively. The GAMMA 10 has MHD anchors with the minimum-B field configuration and is arranged to be effectively axisymmetrized configuration. The axisymmetrization of the heating system is the most important subject on the mirror experiments in relation to the radial particle transport. The improvement of ICRF antenna systems has been performed because the antenna configuration in the central cell affects the plasma profile in the azimuthal

direction [3].

The realization of the high beta plasmas in the central cell is another important issue. The hot ion mode has been appeared and the ion temperature has reached at 10 keV when the strong ICRF heating is applied in the central cell [4]. In such a mode of operation, the plasmas with a strong temperature anisotropy are confined magnetically. In the high beta plasmas with the strong anisotropy, the Alfvén ion cyclotron (AIC) modes are excited spontaneously. The plasma confinement will be affected from the externally applied RF waves and also spontaneously excited waves in the plasma. Occasionally, the saturation of the density and the diamagnetism is observed when the power of ICRF is increased. The magnetic mirror configuration is common in the toroidal devices and also in the space

Corresponding author's e-mail: ichimura@prc.tsukuba.ac.jp

plasmas. In this manuscript, the experimental observations in relation to the particle transport in the axial direction are described.

In the next chapter, the experimental setup is briefly indicated, and characteristics of the AIC modes and the possibility of the control of the AIC modes are described in Chap. 3. In Chap. 4, the effects of AIC modes on the particle transport are indicated and the summary is in Chap. 5.

2. Experimental setup

In the GAMMA 10 tandem mirror, three ICRF sources (RF1, RF2 and RF3) are used in the central cell for the initial plasma production and heating. The initial plasma is produced by using short-pulse plasma guns (1 msec) and applying an ICRF pulse (RF1) with hydrogen gas puffings. Fast Alfvén waves excited by RF1 in the central cell propagate to the anchor cells which are neighboring on both sides of the central cell. These fast Alfvén waves are converted to slow waves in the transition region between the central and anchor cells [5,6] and heat ions in the anchor cell. The magnetic field strength in the anchor cell is adjusted so that the fundamental cyclotron resonance layer exists at the midplane for keeping MHD stabilization. The antennas for RF1 are so-called Nagoya Type III antennas and installed at both east and west ends of the central cell. To avoid the strong interference between east and west antennas, the frequency of the west RF1 antenna (10.3 MHz) is slightly higher than the frequency of the east antenna (9.9 MHz). For the ion heating (RF2), the conventional double half-turn antennas, DHT, are placed inside of the RF1 antennas. Slow Alfvén waves excited by RF2 (6.36 MHz) propagate to the midplane of the central cell and heat ions because the fundamental ion cyclotron resonance layer exist near the midplane. Recently, an ICRF system (RF3) for launching high harmonic fast waves has been constructed. RF3 with a frequency of 63 MHz is successfully used for the higher density plasma production [7]. Typical input powers of RF1 and RF2 are around 200 kW and that of RF3 is below 100 kW. The magnetic field profile in the central and anchor cells, locations of ICRF antennas and the frequencies of RF1, RF2 and RF3 normalized by the local ion cyclotron frequency are indicated in Fig. 1. The strength of the magnetic field at the midplane of the central cell is 0.4 T and the mirror ratio is 5 in the standard mode of operation. A limiter with a diameter of 0.36 m is set near the midplane.

The temperature anisotropy is evaluated from three

diamagnetic loops arrayed in the axial direction in the central cell. Electrostatic and magnetic probes are set in both axial and azimuthal directions for measuring the density and magnetic fluctuations, respectively. To measure the behavior of high energy ions, two diagnostics with semiconductor detectors are installed on the east end (east end High Energy-ion Detector: eeHED) for the end-loss ions and at the midplane of the central cell (central cell HED: ccHED) for the magnetically trapped ions. The structure of eeHED and the sensitivity of the semiconductor detector for protons are described in ref. 8. The ccHED is inserted perpendicularly to the magnetic field line and is positioned just outside of the limiter radius. By rotating the ccHED against the normal axis to the magnetic field line, a pitch angle distribution of high energy ions in the central cell can be measured [9]. High energy ions which are produced by a fundamental cyclotron heating are mainly trapped in the magnetic mirror field of the central cell. The minimum energy of the detection is roughly estimated to be around 10 keV.

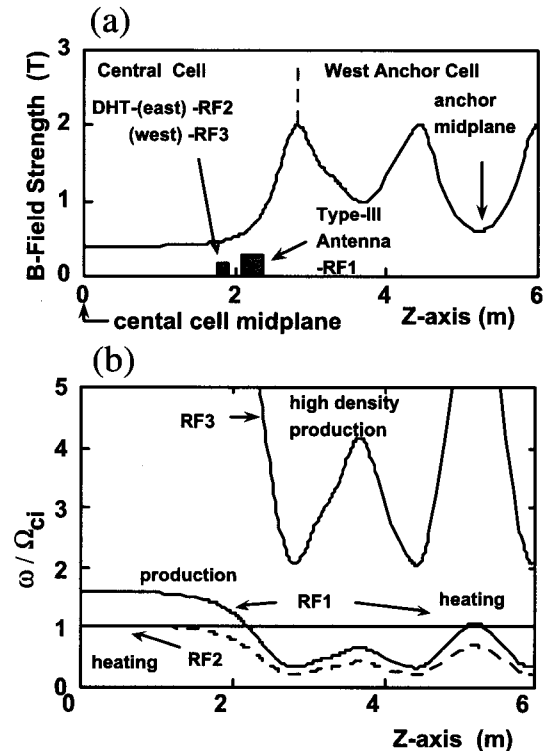


Fig. 1 (a) Magnetic field profile and location of ICRF antennas, (b) Frequencies of RF1, RF2 and RF3 normalized by the local ion cyclotron frequency.

3. Experimental results

3.1 Excitation of AIC modes in plasmas with a strong temperature anisotropy

In the case of a strong ICRF heating with the input power of RF2 up to 250 kW, plasmas with the ion temperature of more than 10 keV have been achieved. Because the cyclotron resonance layer exits near the midplane of the central cell, the temperature anisotropy, $A=T_{\perp}/T_{\parallel}$, which is defined as a ratio between temperatures in the perpendicular, T_{\perp} , and parallel, T_{\parallel} , directions to the magnetic field line, becomes more than 10. The Alfvén ion cyclotron (AIC) modes are spontaneously excited in such high beta, β , plasmas with the strong temperature anisotropy. In GAMMA 10, magnetic fluctuations due to the AIC modes have been observed experimentally in the parameter range of $\beta A^2 > 0.3$. The discrepancy from the theoretical prediction of $\beta A^2 > 3.54$ [10] has been explained by the pressure distribution in the axial direction [11]. As indicated in Fig. 2(a), signals of diamagnetic loops located at the midplane and at $z=1.5$ m from the midplane increase with time and the differences between both signals indicate the anisotropy as shown in Fig. 2(b). When the diamagnetism at the midplane reaches a threshold value, the AIC modes appear. In Fig. 2(b), the total amplitude of the magnetic fluctuations which are detected by a magnetic probe in the AIC frequency range is plotted. The anisotropy becomes more than 10. Figure 3 shows a frequency spectrum of the magnetic probe signal. The peak of 6.36 MHz which corresponds to the ion cyclotron frequency near the midplane of the central cell is externally applied frequency for the plasma heating. Just below the 6.36 MHz peak, several discrete peaks are observed. These peaks indicate the excitation of axial eigenmodes which are determined by the plasma pressure profile in the axial direction. The number of the peaks and the amplitude of each peak depend on the plasma parameters. By changing the magnetic field strength under the fixed frequency, the location of the resonance layer is varied resulting in the change of the anisotropy. Figure 4(a) shows the anisotropy as a function of the diamagnetism for typical two cases of the magnetic field strength. In the low magnetic field case, the strength of the magnetic field is reduced to 97% of the standard operation. Figure 4(b) shows the amplitude of the AIC modes as a function of the anisotropy. On both cases the value of the diamagnetism is fixed to be same as indicated in the figure. The amplitude of the AIC modes becomes small clearly in the low magnetic field case, that is, the

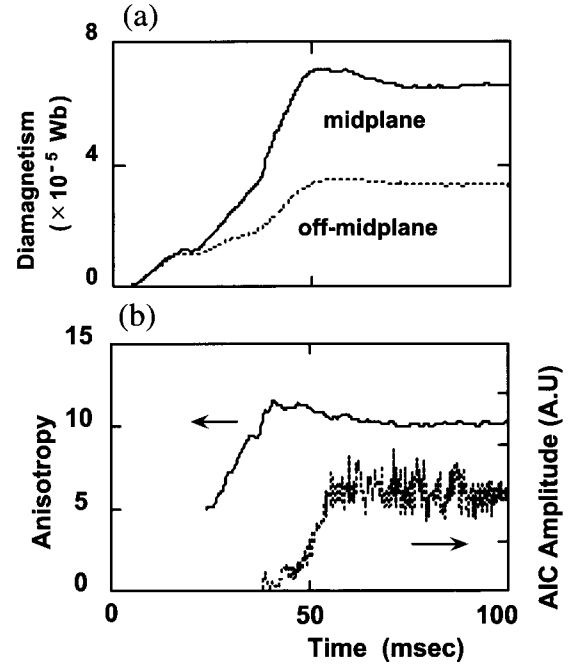


Fig. 2 (a) Signals of diamagnetic loops located at the midplane and off-midplane, (b) Temporal evolution of estimated anisotropy and amplitude of the AIC modes.

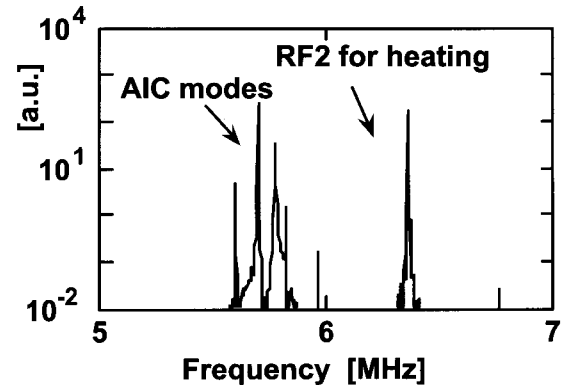


Fig. 3 Frequency spectrum of the magnetic probe.

resonance layer is located in the off-midplane.

3.2 Effects of AIC modes on the particle transport

The drive force of the AIC modes is the anisotropic energy distribution of ions. Then, the behavior of the plasma in the central cell is affected from the excitation of the modes. Figure 5 shows temporal evolution of the line density, the diamagnetism and the amplitude of AIC

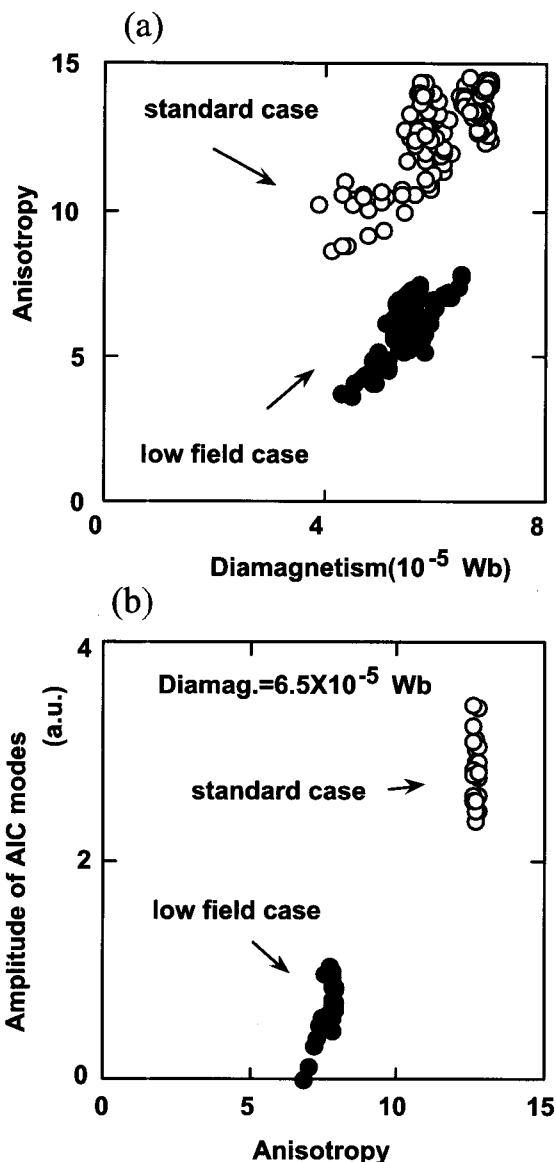


Fig. 4 (a) Anisotropy as a function of diamagnetism in both standard and low field cases, (b) Amplitude of the AIC modes as a function of the anisotropy under the fixed diamagnetism conditions.

modes. The amplitude of AIC modes is plotted as a trace from the top of figure to the bottom in an arbitrary unit. In a start-up period, the density increases and the temperature also increases as indicated in the figure. The start-up of the GAMMA 10 plasma depends strongly on the anchor formation for the MHD stabilization [12]. After build-up of the anchor plasma, the central cell plasmas start to increase and are heated by applying RF2 pulse. In addition to the plasma production with the gas puffing near the RF1 antennas, the trapping of

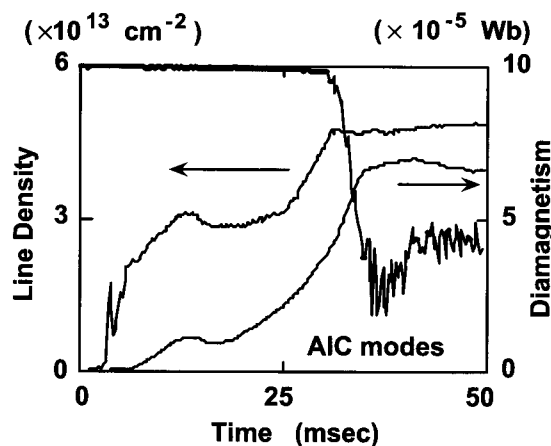


Fig. 5 Temporal evolution of line density, diamagnetism and amplitude of the AIC modes.

passing particles due to the acceleration in the perpendicular direction contributes to the increase in the density. When the diamagnetism reaches at the threshold value and the AIC modes appear, the increasing rate of the density becomes small or sometimes zero. It suggests the number of particles trapped magnetically in the central cell stops to increase and the axial transport of the bulk ions into the loss region is enhanced. The anisotropy also becomes stronger with the diamagnetism. When the AIC modes appear, the anisotropy saturates even if the diamagnetism still increases.

The resonant interaction between electrons and the AIC modes has been also observed in the experiments. By using a multigrid type energy analyzer installed on the end, electrons escaping from the confinement region are detected. In Fig. 6, the temporal evolution of the diamagnetism, the amplitude of the AIC modes and the signal of the end-loss electron flux are indicated. The amplitude of AIC modes is plotted as in Fig. 5. The stepwise increase in the end-loss electron flux with the appearance of the AIC modes are clearly observed. In GAMMA 10, the power from ICRF sources is absorbed directly by ions. The electrons are heated mainly due to the drag from such hot ions. The enhancement of the electron flux in Fig. 6 can not be explained by the increase of the electron drag power and the existence of the additional electron Landau damping of the AIC modes has been suggested [13]. By analyzing energy distributions of electrons on both just before and after AIC modes excitation, the clear increase of the electron temperature is observed.

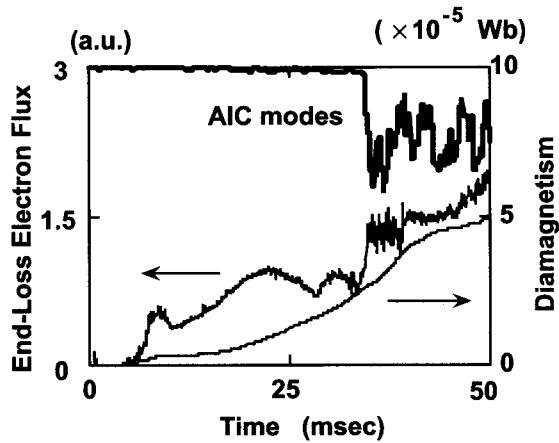


Fig. 6 Temporal evolution of diamagnetism, end-loss electron flux and amplitude of the AIC modes.

The resonant interaction between bulk ions and the AIC modes has been discussed in ref. 14. The effects of the AIC modes on the particle transport have been observed clearly in the behavior of the high energy ions. Figure 7 shows the signals of high energy ion detectors on both perpendicular (ccHED) and parallel (eeHED) directions. In Fig. 7(a), the temporal evolution of both signals and the amplitude of the AIC modes are indicated. The amplitude of AIC modes is plotted as in Fig. 5. The signal of the ccHED increases with an increase in the diamagnetism until 50msec due to the heating. The AIC modes appear at 30msec and the amplitude also increase. When the amplitude of the AIC modes becomes strong, the ccHED signal begins to decrease though the diamagnetism is still increasing. While, the eeHED signal increases clearly with the increase of the amplitude of the AIC modes as shown in Fig. 7(a). It is seen the behaviors of magnetically trapped ions and escaping ions are out of phase. Figure 7(b) shows the signals on the pitch angles of 90, 75 and 60 degrees. The signals on the smaller pitch angles (75 and 60 degrees) are smaller than the signals on the large pitch angle. It indicates that the axial pressure distribution of the ions in the central cell becomes strongly anisotropic. The signals of the small pitch angles tend to increase slightly though the signals of the large pitch angles decrease with an increase of the AIC modes. The behavior of ions with the small pitch angle is the same as that in the end region. These behaviors on the various pitch angles suggest the enhancement of the pitch angle scattering of ions in the velocity space. The axial transport of the high energy ions due to the AIC modes is clearly observed. The mechanism of such a

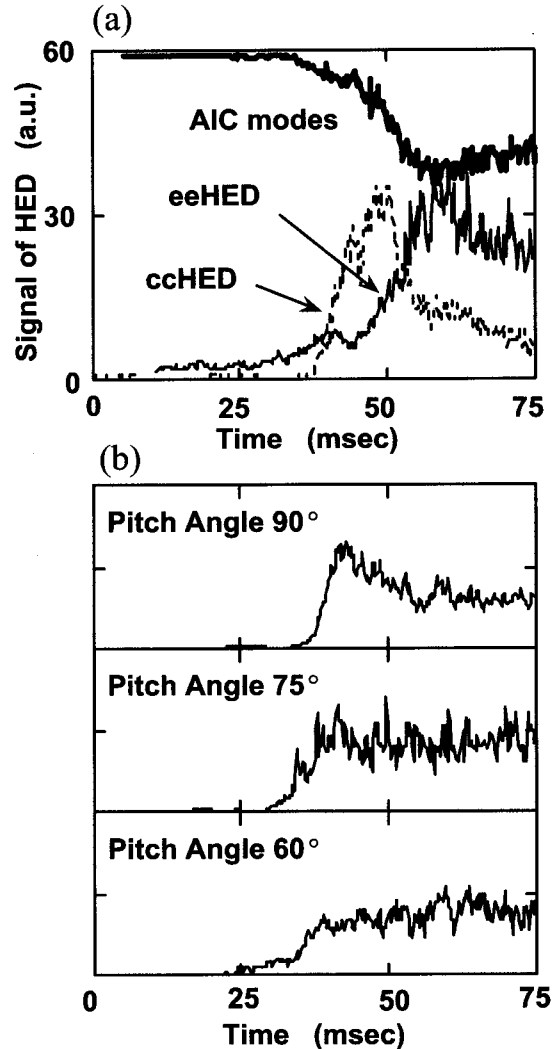


Fig. 7 (a) Temporal evolution of signals of ccHED and eeHED and amplitude of the AIC modes, (b) signals of ccHED on pitch angles of 90, 75 and 60 degrees.

larger pitch angle scattering due to spontaneously excited waves are unknown. It is suggested that the AIC modes excitation restricts the increase in the plasma parameters on future tandem mirror experiments.

4. Summary

In the GAMMA 10 tandem mirror, the Alfvén ion cyclotron (AIC) modes are studied in relation to the particle transport in the axial direction. The AIC modes are shown to be controlled by changing the resonance conditions of the ion cyclotron heating. A resonant interaction between electrons and the AIC modes is observed and the electron Landau damping is strongly

suggested. Pitch angle scattering of high energy ions trapped magnetically in the central cell and the enhancement of the end loss high energy ions are also observed clearly when the AIC modes are excited spontaneously.

References

- [1] K. Yatsu *et al.*, Nucl. Fusion **39**, 1707 (1999).
- [2] K. Yatsu *et al.*, Nuc. Fusion **41**, 613 (2001).
- [3] M. Ichimura *et al.*, Nucl. Fusion **39**, 1995 (1999).
- [4] T. Tamano *et al.*, Proceedings of 15th International Conference on Plasma Physics and Controlled Nuclear Fusion Research, Seville, 1994, (IAEA, Vienna), **2**, 399 (1995).
- [5] M. Inutake *et al.*, Phys. Rev. Lett. **65**, 3397 (1990).
- [6] H. Hojo *et al.*, Phys. Rev. Lett. **66**, 1866 (1991).
- [7] M. Ichimura *et al.*, Phys. Plasmas **8**, 2066 (2001).
- [8] T. Saito *et al.*, Rev. Sci. Instrum. **68**, 1433 (1997).
- [9] M. Ichimura *et al.*, Rev. Sci. Instrum. **70**, 834 (1999).
- [10] G.R. Smith, T.A. Casper and M.J. Gerver, Nucl. Fusion **23**, 1381 (1983).
- [11] M. Nakamura *et al.*, Trans. Fusion Technol. **39**, 394 (2001).
- [12] M. Ichimura *et al.*, Nucl. Fusion **28**, 799 (1988).
- [13] T. Saito *et al.*, Phys. Rev. Lett. **82**, 1169 (1999).
- [14] K. Ishii *et al.*, Phys. Rev. Lett. **83**, 3438, (1999).